International Journal of Minerals, Metallurgy and Materials
Volume 26, Number 4, April 2019, Page 460
https://doi.org/10.1007/s12613-019-1753-5

Segmented tubular synthesis of monodispersed microsized copper oxalate

Xun Liu[1)], *Xing Chen*[1,2)], *and Kai Huang*[1,2)]

1) School of Metallurgical and Ecological Engineering, University of Science and Technology Beijing, Beijing 100083, China

2) Beijing Key Lab of Green Recycling and Extraction of Metals, University of Science and Technology Beijing, Beijing 100083, China

(Received: 6 July 2018 revised: 8 September 2018; accepted: 13 September 2018)

Abstract: Monodispersed microsized copper oxalate particles were prepared in a segmented continuous flow tube reactor, and the effect of the main parameters such as organic additive agent, initial copper ions concentration, residence time, and segmented media on the final products were investigated experimentally. The obtained copper oxalate microsized particles were disc-like in the presence of citrate ligand, which was the shape inducer for the precipitated copper oxalate. Thermodynamic equilibrium diagrams of the Cu(II)–oxalate–H_2O, Cu(II)–oxalate–citrate–H_2O, and Cu(II)–oxalate–EDTA–H_2O solution systems were drawn to estimate the possible copper species under the experimental conditions and to explain the formation mechanisms of copper oxalate particles in the segmented fluidic reactor. Both theoretical and experimental results indicated that the presence of chelating reagents such as citrate and EDTA had distinct effect on the evolution of particle shape. Air and kerosene were tested as media for the fluidic flow segmentation, and the latter was verified to better promote the growth of copper oxalate particles. The present study provides an easy method to prepare monodispersed copper oxalate microsized particles in a continuous scaling-up way, which can be utilized to prepare the precursor material for conductive inks.

Keywords: segmented flow tube reactor; copper oxalate powder; monodispersed; scaling-up; shape inducer

1. Introduction

Conductive inks have been widely studied in recent years because of their popularity in the industries of printed electronics (PE) and flexible electronics (FE) [1]. Their usage has been found to be unique and noncompetitive in a completely new frontier of future technologies [2]. Silver is a typical metal that is keenly investigated for its promising applications in conductive inks because of its excellent conductivity and resistance to the oxidation [3]. In printing technology, silver conductive inks play a major role in electronic applications and attract much attention [4–6]; however, silver inks are costly [7]. To overcome this drawback, copper conductive inks are regarded as an alternative to the current silver-based materials [8]. Although copper ink is much cheaper, a major challenge in using copper ink is its poor resistance to the oxidation during storage and sintering [9–11]. Recently, decomposable copper compounds have been used as the precursor material for e-inks synthesis [12]; and printing circuit boards were fabricated by a sequential thermolysis treatment to transfer the copper compounds into copper metal lines in a protective atmosphere of inert gas [13–14]. Precursor-based copper conductive inks have a great potential of substituting the traditional printing circuit board technology because of their fabrication convenience and less manufacturing cost [15]. Because of the prominent advantages of copper inks in the electronic industry, many researchers have studied the application of this technology in printed electronics industries [16]. Among the groups of various copper compounds, copper oxalate has unique merits because of its good crystalline phase and regular shapes during the synthesis process through wet-chemical methods [17]. In addition, copper oxalate easily undergoes direct thermal decomposition in a protective atmosphere to yield copper particles ($CuC_2O_4{\cdot}2H_2O \rightarrow Cu + 2CO_2 + 2H_2O$). The size and dispersity of the copper oxalate particles are the main parameters to determine the suspension stability of the inks; therefore, the synthesis of monodispersed ultrafine copper oxalate particles is quite essential to the final quality of the printing circuit boards. To prepare the monodispersed particles by wet precipitation processes on a large scale, a segmented flow tube reactor is proposed in the present study,

Corresponding author: Kai Huang E-mail: khuang@metall.ustb.edu.cn

and the feasibility of copper oxalate powder as the precursor material in the preparation of conductive ink for electronic applications is preliminarily studied. The use of segmented fluidic reactor for the preparation of fine inorganic particles has been widely studied [18–20] because of its prominent merits such as excellent homogeneous mixing, good reaction stability, good reproducibility, and easy scaling-up [21–22]. However, to the best of our knowledge, the preparation of monodispersed copper oxalate particles in a segmented fluidic reactor is seldom reported. Thus, in the present study, we designed a synthesis system for the scaling-up preparation of copper oxalate particles, and the relative mechanisms are discussed based on a thermodynamic equilibrium calculation of the related solution systems.

2. Experimental

2.1. Chemicals

Copper sulfate ($CuSO_4$), sodium oxalate ($Na_2C_2O_4$), polyvinylpyrrolidone (PVP), sodium citrate, and ethylenediaminetetraacetic acid (EDTA) reagents were purchased from Sinopharm Chemical Reagent Co. Ltd., China), and all the regents were analytically pure and were used as received without further purification.

2.2. Synthesis of monodispersed copper oxalate particles

Fig. 1 demonstrates a basic schematic diagram of a segmented flow tube reactor. In this study, 0.1 mol/L copper sulfate with 5 g/L PVP and 0.1 mol/L sodium oxalate with 5 g/L PVP were prepared as the stock solutions. Then, they were simultaneously fed to a polypropylene (PP) tube (ϕ3 mm × 1 m) by a Y-type mixer (the intersection angle for two feeding conducts is 60°) at 5 mL/min, and a flow of air into the mixing solution was used to segment the solution into a separate 0.3 cm long liquid phase, in which precipitation spontaneously occurred. When the segmented solution jetted out of the tube, the suspension was collected in a large beaker with alcohol, which completely diluted the solution to stop the precipitation reaction, and the solution was kept to age a certain period while being stirred. Samples

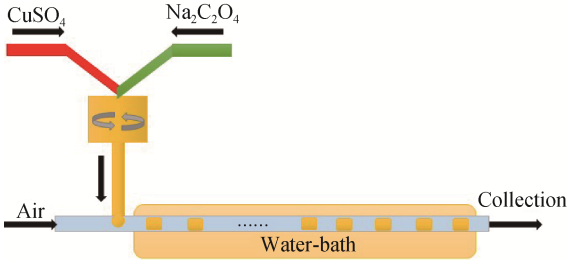

Fig. 1. Schematic diagram of a segmented continuous flow tube reactor.

were taken after a period of time for centrifugation. The grey blue products were isolated, cleaned by three cycles of centrifugation, washed, redispersed in alcohol, and oven-dried at 60°C for 8 h.

2.3. Characterization

Field-emission scanning electron microscopy (SEM) observation was carried out using a FEI Sirion field-emission gun scanning electron microscope operated at 25 keV. The samples for SEM observation were prepared by depositing dried copper oxalate particles on a silicon stand followed by gold spraying. The UV-Visible absorption spectra were acquired using a Shimadzu 2450/2550PC spectrophotometer equipped with an integrating sphere attachment. An X-ray diffraction (XRD) analysis was carried out to identify the phase compositions for the samples on a Rigaku-6000 XRD instrument.

3. Results and discussion

3.1. Effect of additive agent

The copper oxalate particles prepared using a segmented flow tube reactor in the absence of any additives were almost perfectly spherical as demonstrated in the SEM image of the copper oxalate particles (Fig. 2(a)), and the average diameter is about 2 μm. The image indicates that the morphology of the copper oxalate particles is perfectly spherical, and their surfaces have some cracks. When citrate ligand additive was added, the spherical particles became disk-like (Fig. 2(b)). The citrate acted as a shape inducer for the copper oxalate precipitate. However, when additive agents PVP and EDTA were added, the copper oxalate particles remained spherical. Therefore, the additive agents had different effects on the shape evolution of the precipitated particles.

X-ray diffraction analysis and Fourier transform infrared (FTIR) spectroscopy tests were conducted on the obtained copper oxalate particles, and the results were illustrated in Figs. 3 and 4. As indicated in Fig. 3, all the obtained particles were of pure dihydrate copper oxalate phase, while from the strongest peak of <110>, it can be found that different additives exhibited significant individual effect on the intensity of the copper oxalate phase. The XRD pattern indicates that citrate and EDTA inhibited the growth of <110> crystal facet, while PVP promoted it. Considering the molecular compositions of PVP ($(C_6H_9NO)_n$), citrate (C_3H_5O–3COOH), and EDTA ($C_6H_{12}N_2$–4COOH), citrate and EDTA can coordinate with copper ions, while PVP cannot. Therefore, the chelating effect of citrate or EDTA with the copper ions might have played an indispensable role in the inhibition of the crystal facet <110> growth.

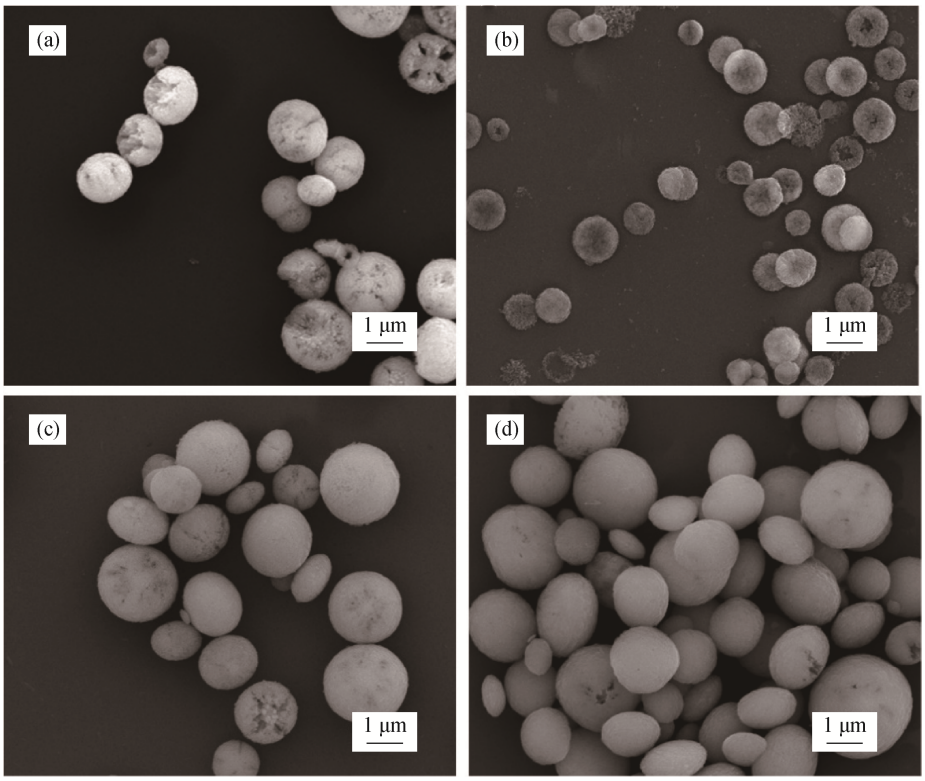

Fig. 2. SEM images of copper oxalate particles obtained in an air-segmented fluidic reactor by simultaneous feeding of 0.1 mol/L Cu(II) and 0.1 mol/L sodium oxalate solutions for a residence time period of 10 min in the absence of surfactant (a) and in the presence of 5 g/L sodium citrate (b), 5 g/L PVP (c), and 5 g/L EDTA (d).

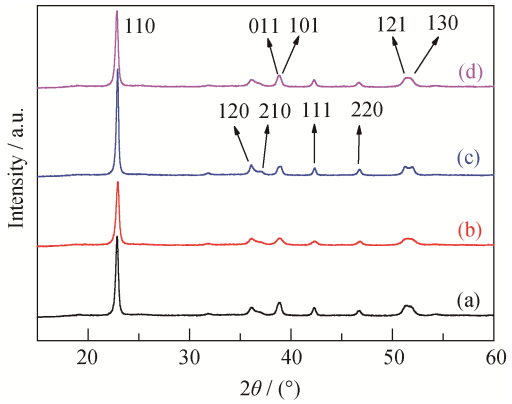

Fig. 3. XRD patterns of copper oxalate particles obtained in an air-segmented fluidic reactor by simultaneous feeding of 0.1 mol/L Cu(II) and 0.1 mol/L sodium oxalate solutions for a residence time period of 10 min in the absence of surfactant (a) and in the presence of 5 g/L sodium citrate (b), 5 g/L PVP (c), and 5 g/L EDTA (d).

The FTIR results are shown in Fig. 4, and they provide more information about the four samples. The FTIR spectrum for the copper oxalate solution with PVP has weak peaks near 1613, 1363, and 1319 cm^{-1}; these peaks can be ascribed to the stretch vibration of –COOH ligands. The stronger peaks at 823 and 505 cm^{-1} correspond to the vibration of Cu–O bonds. Citrate and EDTA both had opposite effects that resulted in weak –COOH and Cu–O peaks. The chelating effect of citrate and EDTA was confirmed to have the major influence on the crystal growth behavior of copper oxalate particles as well as their morphological evolution.

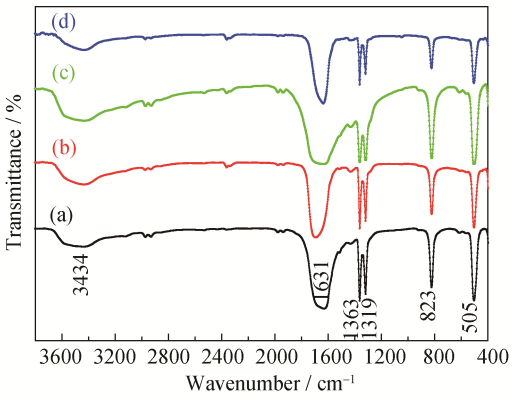

Fig. 4. FTIR curves of copper oxalate particles in an air-segmented fluidic reactor by simultaneous feeding of 0.1 mol/L Cu(II) and 0.1 mol/L sodium oxalate solutions for a residence time period of 10 min in the absence of surfactant (a) and in the presence of 5 g/L sodium citrate (b), 5 g/L PVP (c), and 5 g/L EDTA (d).

3.2. Effect of initial copper concentration

Fig. 5 shows the SEM images of copper oxalate particle samples obtained under different initial concentrations of copper and oxalate. It can be seen that a lower concentration of copper ions favors the dispersion of the copper oxalate particles, and a concentration of 0.05 mol/L copper ions is recommended for better monodispersity, as shown in Fig. 5. Although the yield of particles in the low concentration is not large, the morphology and size uniformity are usually rather satisfactory. Considering that the properties of the particles are strongly dependent on their monodisperse size distribution and morphology, a low concentration of the feeding solutions should be selected for the particles synthesis; otherwise, a large number of particles would be produced, but the corresponding properties would be poor. Such trade-off between quantity and quality in the monodispersed particles preparation is a core challenge.

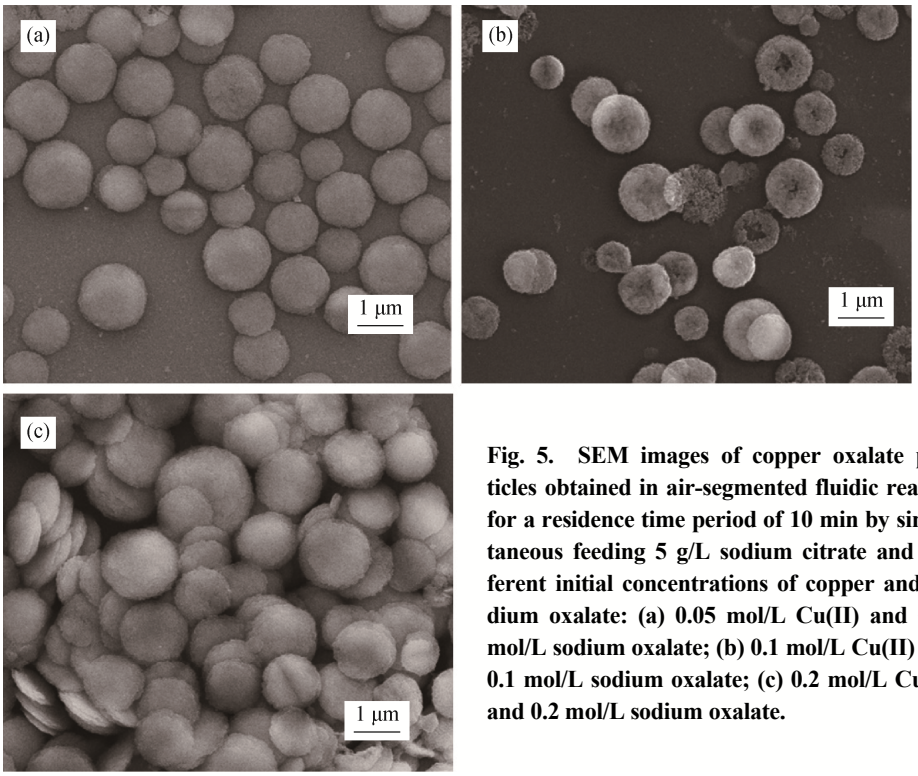

Fig. 5. SEM images of copper oxalate particles obtained in air-segmented fluidic reactor for a residence time period of 10 min by simultaneous feeding 5 g/L sodium citrate and different initial concentrations of copper and sodium oxalate: (a) 0.05 mol/L Cu(II) and 0.05 mol/L sodium oxalate; (b) 0.1 mol/L Cu(II) and 0.1 mol/L sodium oxalate; (c) 0.2 mol/L Cu(II) and 0.2 mol/L sodium oxalate.

3.3. Effect of reaction time

Fig. 6 shows SEM images of the copper oxalate particles obtained for different reaction or residence time periods. With an increase in residence time, the spherical copper oxalate particles becomes smoother, but the dispersity worsens; this may be due to the more interfering factors involved in the growth process with increased residence time. 10 min is recommended as the suitable residence time, as it resulted in the production of acceptable monodispersed disc-like copper oxalate particles.

3.4. Effect of segmentation media

Fig. 7 shows the copper oxalate particles images obtained under different segmentation media: air and kerosene. In the experiment, it was found that for kerosene segmentation, the inner wall of the fluidic PP tube was very clean and smooth, while for air segmentation, the inner wall was dirty with the deposition of copper oxalate fine particles. This is probably due to the excellent wettability of kerosene with PP, which led to the homogenous formation of a very thin kerosene liquid layer on the inner wall surface of the PP tube, preventing the deposition of copper oxalate precipitates. When air was used as the segmentation media, the PP tube inner wall did not form gas film; thus, it was difficult to avoid the deposition of precipitates. In addition, the copper oxalate particles obtained under the kerosene segmentation seemed to be compacter and smoother than those obtained under air segmentation. This may be related with the more static precipitation conditions in the kerosene-segmented fluidic liquid phase.

3.5. Formation mechanism of monodispersed copper oxalate

The above results indicate that the presence of chelating reagents significantly influences the morphology and size of

the precipitated dihydrate copper oxalate particles. The formation mechanisms of the precipitates under the different conditions are still unclear. However, it has been well recognized that the main properties and characteristics of the solution are strongly and directly responsible for the precipitation processes.

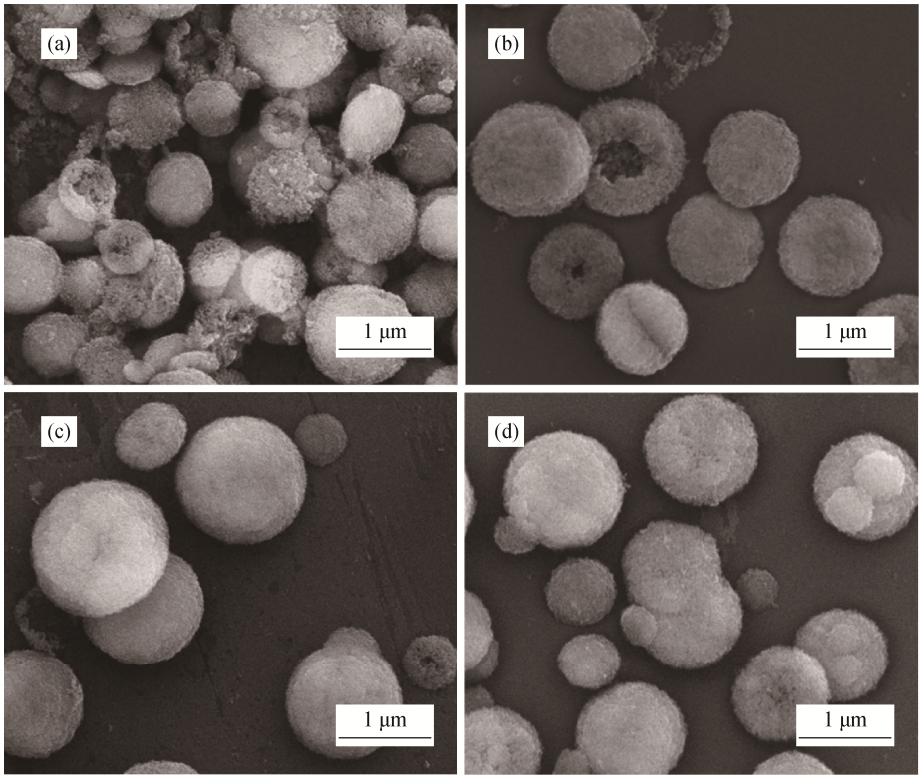

Fig. 6. SEM images of copper oxalate particles obtained in air-segmented fluidic reactor by simultaneous feeding of 0.1 mol/L Cu(II) with 5 g/L sodium citrate and 0.1 mol/L sodium oxalate with 5 g/L sodium citrate for different residence time periods: (a) 5 min; (b) 10 min; (c) 25 min; (d) 50 min.

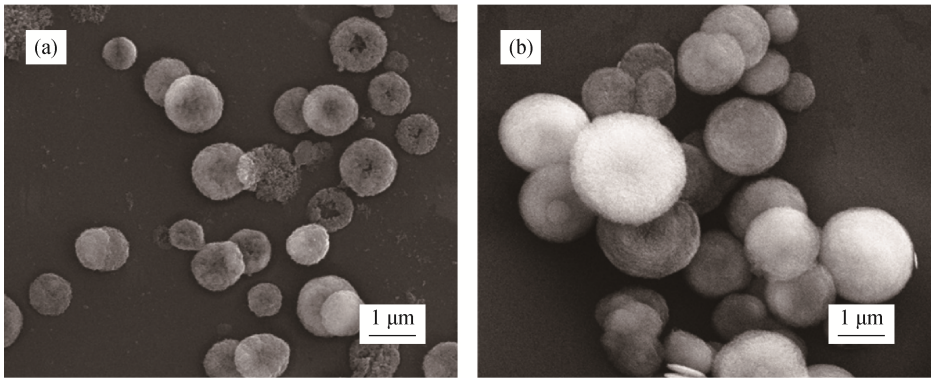

Fig. 7. SEM images of copper oxalate particles obtained in (a) air-segmented fluidic reactor and (b) kerosene-segmented fluidic reactor by simultaneous feeding of 0.1 mol/L Cu(II) with 5 g/L sodium citrate and 0.1 mol/L sodium oxalate with 5 g/L sodium citrate for a residence time period of 10 min.

To clarify the formation mechanisms of the precipitate, the solution compositions and chemical structures should be adequately explored. Based on the above ideas, we determined the copper species in the solution samples according to thermodynamic equilibrium principles [23–24], and the main results are illustrated in Fig. 8.

A mixed solution of 0.1 mol/L Cu(II) and 0.1 mol/L sodium oxalate was the basic sample for study. The copper species were rather simple: copper oxalate at pH below 8, copper hydroxide at pH above 8, and a very small amount of copper oxalate complex at pH 8–10, as shown in Fig. 8(a). It was also verified by experiments that a large quantity of copper oxalate was precipitated at pH near 5.5, after about 30 s induction period for nucleation. In this case, an aliquot

of citrate was introduced in the mixing solution at a concentration of 0.017 mmol/L (5 g/L), and the induction period time was found to prolong to 10 min. The presence of citrate caused the formation of $Cu_2(cit)_2OH^{3-}$ complex as shown in Fig. 8(b), which slowed the precipitation rate of copper oxalate. In more dilute solutions (0.05 mol/L copper ions), the same concentration of citrate caused more drastic effect on the precipitation process, as shown in Fig. 8(c); more $Cu_2(cit)_2OH^{3-}$ was formed, and the induction period for nucleation was much longer (about 25 min). For comparison, a more concentrated copper ion solution (0.20 mol/L) was used as the precipitating agent; less $Cu_2(cit)_2OH^{3-}$ was produced because of the stronger precipitation effect of the higher copper ion concentration, and 2.5 min was enough for precipitation to occur (Fig. 8(d)). In addition, for comparison, under the same copper and oxalate concentrations used for the citrate experiment, EDTA was used to evaluate the copper species distribution because of its much stronger chelating capability with copper ions than that of citrate. More copper complexes of EDTA were produced in the corresponding pH range (Fig. 8(e)), and it was further verified by experimental results that a longer induction period of 13 min was required for nucleation.

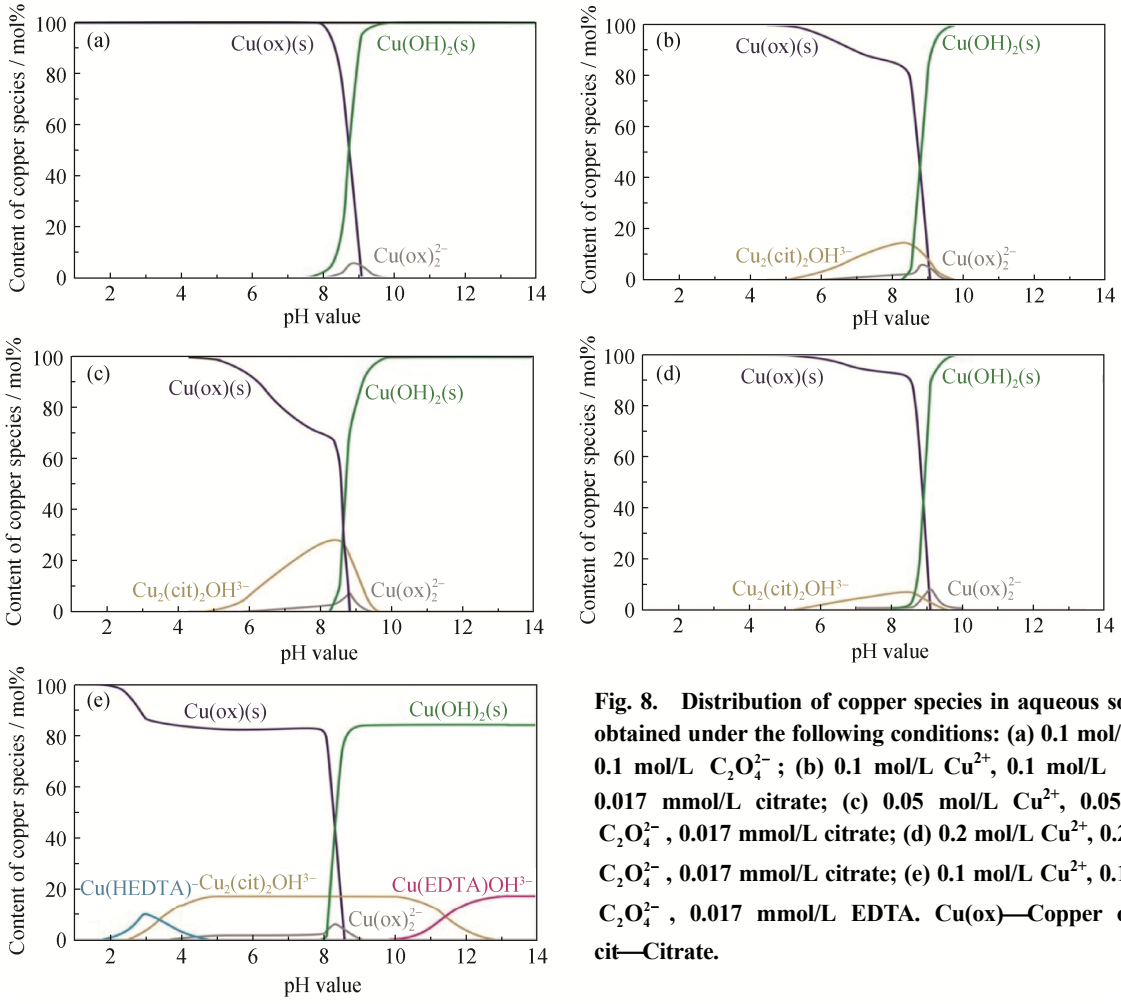

Fig. 8. Distribution of copper species in aqueous solutions obtained under the following conditions: (a) 0.1 mol/L Cu^{2+}, 0.1 mol/L $C_2O_4^{2-}$; (b) 0.1 mol/L Cu^{2+}, 0.1 mol/L $C_2O_4^{2-}$, 0.017 mmol/L citrate; (c) 0.05 mol/L Cu^{2+}, 0.05 mol/L $C_2O_4^{2-}$, 0.017 mmol/L citrate; (d) 0.2 mol/L Cu^{2+}, 0.2 mol/L $C_2O_4^{2-}$, 0.017 mmol/L citrate; (e) 0.1 mol/L Cu^{2+}, 0.1 mol/L $C_2O_4^{2-}$, 0.017 mmol/L EDTA. Cu(ox)—Copper oxalate; cit—Citrate.

It can be deduced that the strong chelating affinity of organic acids with the copper ions led to the different induction periods for nucleation as well as the growth process. The chelating affinity influenced the supersaturation profiles and consequently the nucleation and growth kinetics. In addition, the selective absorption of citrate molecules onto the specific <110> crystal facet caused the variation of orientated growth rate, which affected the final shape of the precipitated particles. Similar results and explanation about the formation of disc-like copper oxalate particles have been reported in Ref. [25]. In summary, the presence of citrate significantly affected the shape and morphology, and the chelating effect and selective absorption of citrate onto the <110> crystal facet are the main factors responsible for the formation of disc-like copper oxalate particles. Therefore, the citrate can be regarded as an effective shape and mor-

phology inducer, which help to tailor the copper oxalate particles via the solution chemical routes as discussed above. Thus, selecting an appropriate solution will favor the synthesis of the fine particles with desirable size and morphology. The segmented tubular reactor has unique advantages in terms of temperature and concentration control; therefore, combining appropriate solution selection and reactor design will lead to the continuous production of a large amount of monodispersed fine particles.

4. Conclusions

Monodispersed dihydrate copper oxalate particles were prepared in a segmented fluidic reactor with a constant reproducibility and good uniformity. Thermodynamic equilibrium calculation demonstrated that Cu(II)–citrate and Cu(II)–EDTA formed in the acidic pH range, and therefore, the induction period for nucleation in the experiments was affected significantly, as well as the nuclei growth process. The chelating effect of citrate and the selective absorption of citrate molecules onto the <110> crystal facet led to the formation of disc-like copper oxalate precipitates.

References

[1] F. Roux, S. Amtablian, M. Anton, *et al.*, Chalcopyrite thin-film solar cells by industry-compatible ink-based process, *Sol. Energy Mater. Sol. Cells*, 115(2013), p. 86.

[2] H. Min, B. Lee, S. Jeong, and M. Lee, Fabrication of 10 μm-scale conductive Cu patterns by selective laser sintering of Cu complex ink, *Opt. Laser Technol.*, 88(2017), p. 128.

[3] C.W. Chang, T.Y. Cheng, and Y.C. Liao, Encapsulated silver nanoparticles in water/oil emulsion for conductive inks, *J. Taiwan Inst. Chem. Eng.*, 92(2018), p. 8.

[4] S. Bose, S. Chakraborty, and D. Sanyal, Water-ethylene glycol mediated synthesis of silver nanoparticles for conductive ink, *Mater. Today Proc.*, 5(2018), No. 3, p. 9941.

[5] J. Kastner, T. Faury, H.M. Außerhuber, *et al.*, Silver-based reactive ink for inkjet-printing of conductive lines on textiles, *Microelectron. Eng.*, 176(2017), p. 84.

[6] Z.H. Wang, W. Wang, Z.K. Jiang, and D. Yu, Low temperature sintering nano-silver conductive ink printed on cotton fabric as printed electronics, *Prog. Org. Coat.*, 101(2016), p. 604.

[7] B.J. De Gans, P.C. Duineveld, and U.S. Schubert, Inkjet printing of polymers: State of the art and future developments, *Adv. Mater.*, 16(2010), No. 3, p. 203.

[8] D. Kim, S. Jeong, and J. Moon, Synthesis of silver nanoparticles using the polyol process and the influence of precursor injection, *Nanotechnology*, 17(2006), No. 16, p. 4019.

[9] T. Öhlund, A.K. Schuppert, M. Hummelgård, J. Bäckström, H.E. Nilsson, and H. Olin, Inkjet fabrication of copper patterns for flexible electronics: Using paper with active precoatings, *ACS Appl. Mater. Interfaces*, 7(2015), No. 33, p. 18273.

[10] Y. Hokita, M. Kanzaki, T. Sugiyama, R. Arakawa, and H. Kawasaki, High-concentration synthesis of sub-10 nm copper nanoparticles for application to conductive nanoinks, *ACS Appl. Mater. Interfaces*, 7(2015), No. 34, p. 19382.

[11] T. Sugiyama, M. Kanzaki, R. Arakawa, and H. Kawasaki, Low-temperature sintering of metallacyclic stabilized copper nanoparticles and adhesion enhancement of conductive copper film to a polyimide substrate, *J. Mater. Sci. Mater. Electron.*, 27(2016), No. 7, p. 7540.

[12] A. Yabuki, Y. Tachibana, and I.W. Fathona, Synthesis of copper conductive film by low-temperature thermal decomposition of copper–aminediol complexes under an air atmosphere, *Mater. Chem. Phys.*, 148(2014), No. 1-2, p. 299.

[13] A. Yabuki, N. Arriffin, and M. Yanase, Low-temperature synthesis of copper conductive film by thermal decomposition of copper–amine complexes, *Thin Solid Films*, 519(2011), No. 19, p. 6530.

[14] A. Yabuki and S. Tanaka, Electrically conductive copper film prepared at low temperature by thermal decomposition of copper amine complexes with various amines, *Mater. Res. Bull.*, 47(2012), No. 12, p. 4107.

[15] D. Adner, F.M. Wolf, S. Möckel, J. Perelaer, U.S. Schubert, and H. Lang, Copper(II) ethylene glycol carboxylates as precursors for inkjet printing of conductive copper patterns, *Thin Solid Films*, 565(2014), p. 143.

[16] Y. Dong, X.D. Li, S.H. Liu, Q. Zhu, M. Zhang, J.G. Li, and X.D. Sun, Optimizing formulations of silver organic decomposition ink for producing highly-conductive features on flexible substrates: The case study of amines, *Thin Solid Films*, 616(2016), p. 635.

[17] A.T. Royappa, A.D. Royappa, R.F. Moral, *et al.*, Copper(I) oxalate complexes: Synthesis, structures and surprises, *Polyhedron*, 119(2016), p. 563.

[18] A. Manz, N. Graber, and H.M. Widmer, Miniaturized total chemical analysis systems: A novel concept for chemical sensing, *Sens. Actuators B*, 1(1990), No. 1-6, p. 244.

[19] J.H. Chun, S. Lu, Y.S. Lee, and V.W. Pike, Fast and high-yield micro-reactor syntheses of *ortho*-substituted [^{18}F]fluoroarenes from reactions of [^{18}F]fluoride ion with diaryliodonium salts, *J. Org. Chem.*, 75(2010), No. 10, p. 3332.

[20] S.J. Haswell, R.J. Middleton, B. O'Sullivan, V. Skelton, P. Watts, and P. Styring, ChemInform abstract: The application of micro reactors to synthesis chemistry, *Cheminform*, 32(2010), No. 23, DOI: 10.1002/chin.200123238.

[21] K. Schubert, J. Brandner, M. Fichtner, G. Linder, U. Schygulla, and A. Wenka, Microstructure devices for applications in thermal and chemical process engineering, *Microscale Thermophys. Eng.*, 5(2001), No. 1, p. 17.

[22] K. Jähnisch, V. Hessel, H. Löwe, and M. Baerns, Chemistry in microstructured reactors, *Angew. Chem. Int. Ed.*, 43(2004), No. 4, p. 406.

[23] M.T. Tang, *Theory and Technology of Complex Metallurgy*, Central South University Press, Changsha, 2011.

[24] X.W. Yang and D.F. Qiu, *Hydrometallurgy*, 2nd Ed., Metallurgical Industry Press, Beijing, 2011.

[25] X.L. Zhou, Z.G. Yan, and X.D. Han, From ascorbic acid to oxalate: Hydrothermal synthesis of copper oxalate microspheres and conversion to oxide, *Mater. Lett.*, 118(2014), p. 39.